

Electronic supplementary information

**In situ coupling strategy for the preparation of
heterometal-doped carbon framework as efficient
bifunctional ORR/OER electrocatalyst**

Hui Li^a, Zhuyin Sui^{*,b}

*^a Department of Chemistry, Key Laboratory of Bioorganic Phosphorus
Chemistry & Chemical Biology, Beijing Key Laboratory for Analytical
Methods and Instrumentation, Tsinghua University, Beijing 100084, China.*

*^b College of Chemistry & Chemical Engineering, Yantai University, Yantai
264005, China*

Tel: +86 535 690 2433

Email: suizhuyin@163.com

Section 1. SEM image

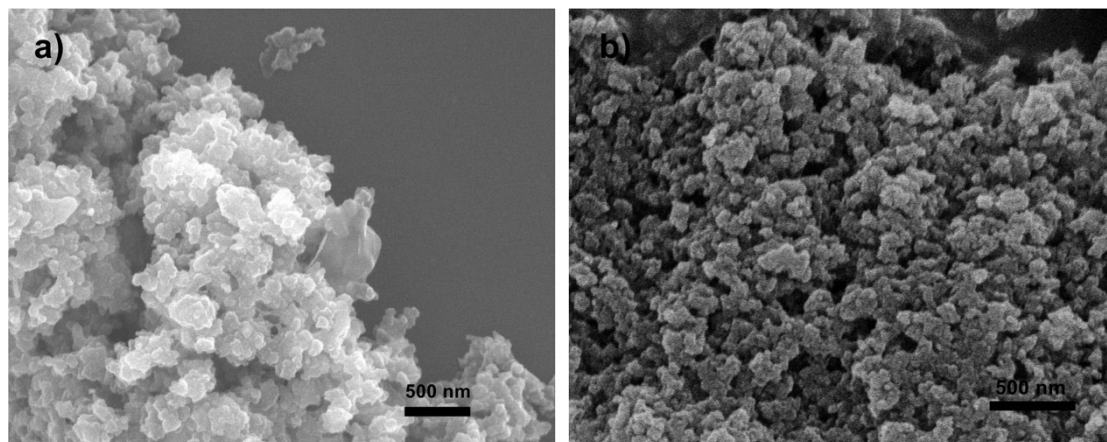


Fig. S1 SEM images of CMP-CoFe/C.

Section 2. FT-IR profile

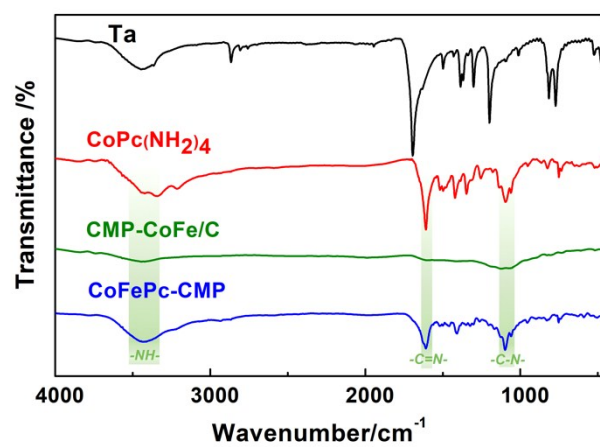


Fig. S2 FT-IR spectra of terephthalaldehyde (TA), CoPc(NH₂)₄, CoFePc-CMP and CMP-CoFe/C.

Section 3. HRTEM image

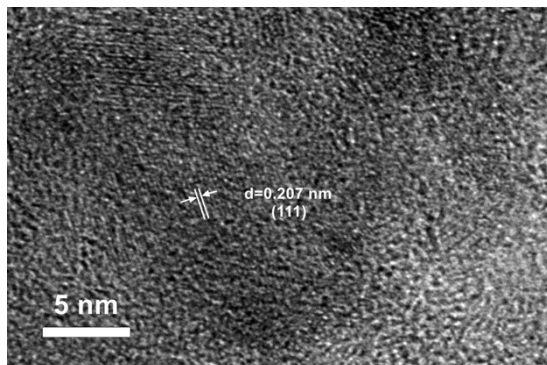


Fig. S3 HRTEM image of Co-N_x in CMP-CoFe/C.

Section 4. Raman spectrum

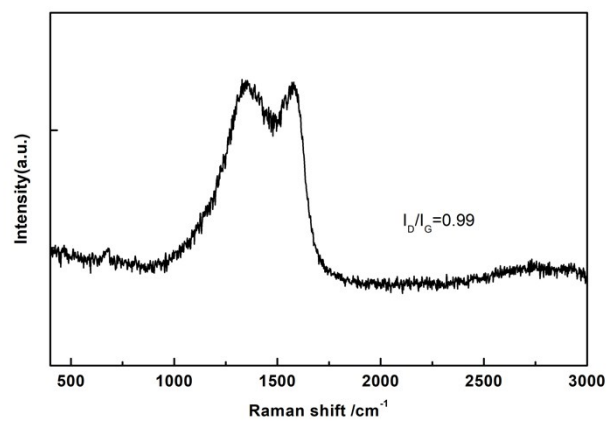


Fig. S4 Raman spectrum of CMP-CoFe/C.

Section 5. BET profile

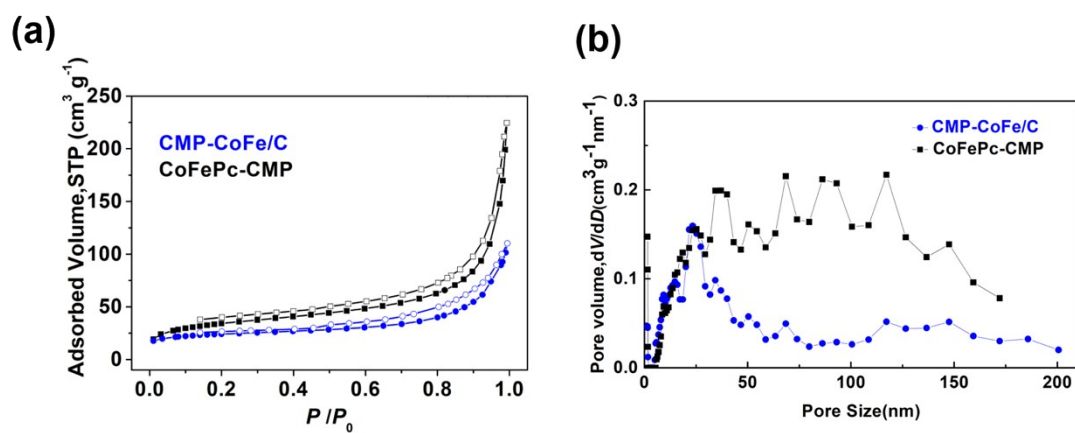


Fig. S5 (a) Nitrogen adsorption-desorption isotherms and (b) pore size distribution of CMP-CoFe/C and CoFePc-CMP.

Section 6. XAFS profile

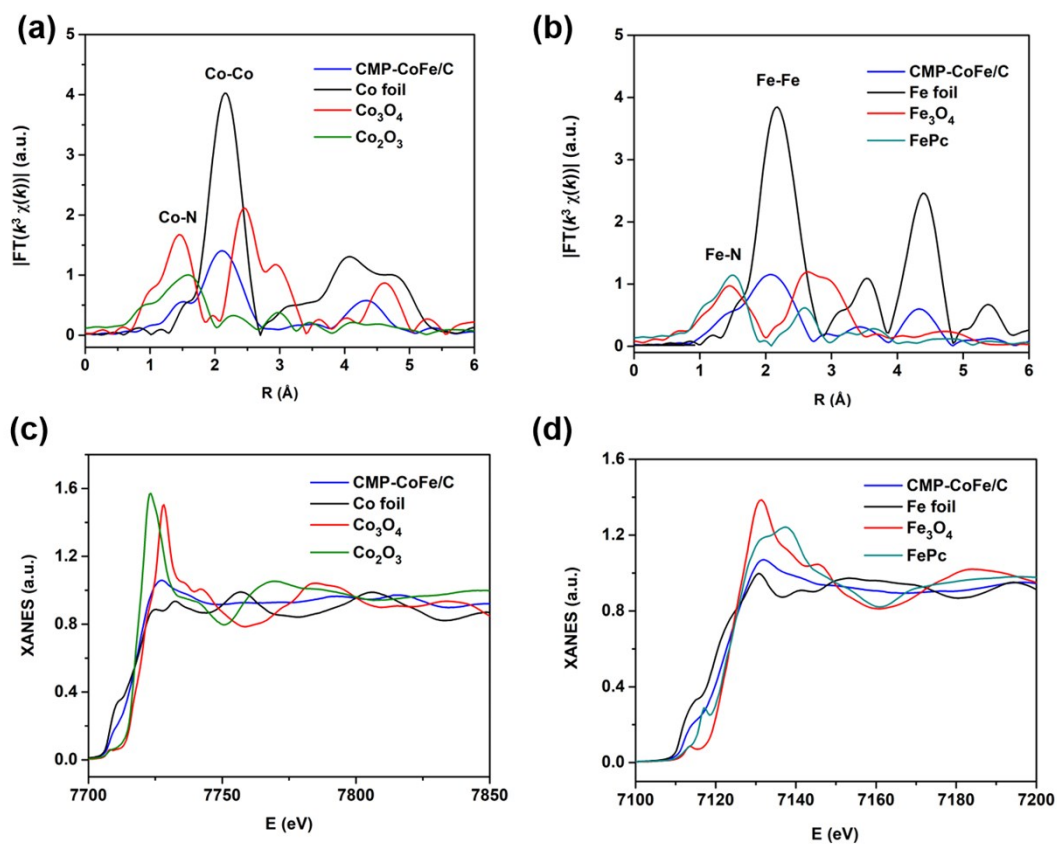


Fig. S6 Fourier transformed k^3 -weighted $\chi(k)$ -function of the EXAFS spectra for (a) Co K-edge and (b) Fe K-edge of CMP-CoFe/C. (c) Co K-edge and (d) Fe K-edge XANES spectra of CMP-CoFe/C.

Section 7. CV curves

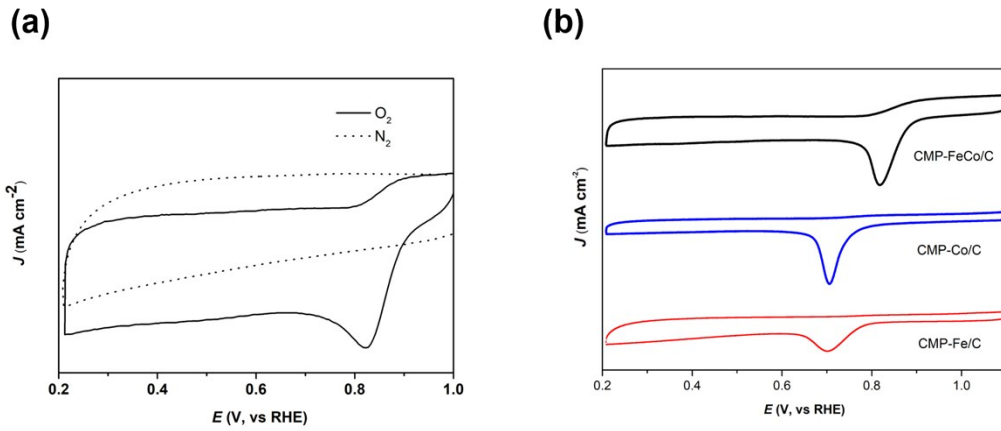


Fig. S7 (a) CV curves of CMP-CoFe/C in N₂- or O₂-saturated 0.1 M KOH aqueous solution. (b) CV curves of CMP-CoFe/C, CMP-Fe/C and CMP-Co/C in O₂-saturated 0.1 M KOH aqueous solution.

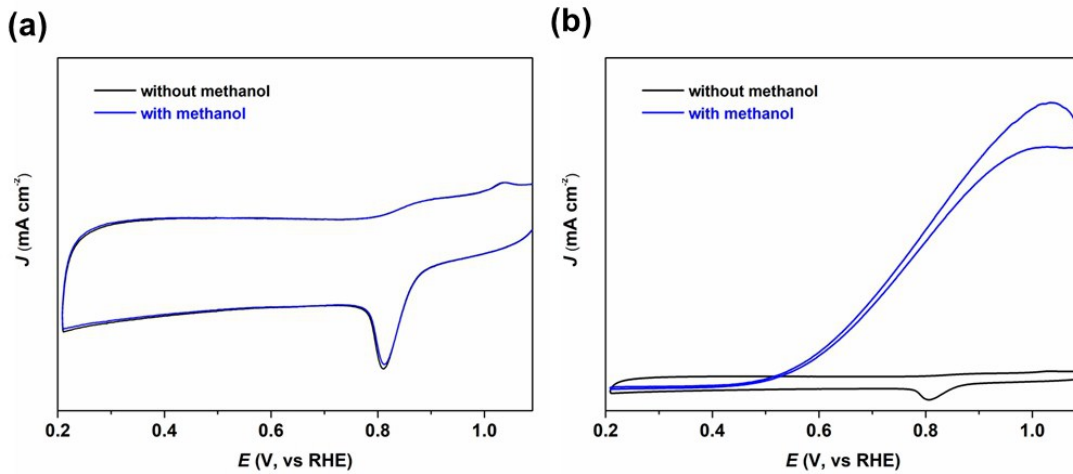


Fig. S8 CV curves of CMP-CoFe/C (a) and 20 wt% Pt/C (b) at a scan rate of 50 mV s⁻¹ in O₂-saturated 0.1 M KOH solution containing 3M methanol.

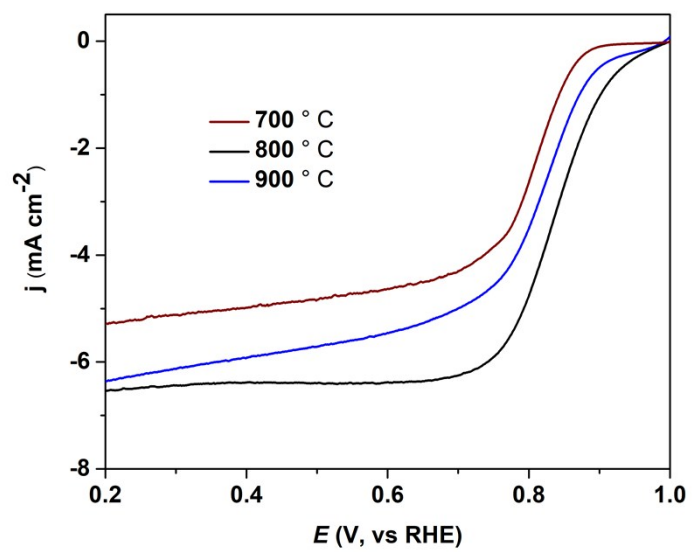


Fig. S9 LSV polarization curves of CMP-CoFe/C obtained by pyrolyzing at 700 °C, 800 °C, and 900 °C.

Section 8. The electrochemically active surface area (ECSA) profile

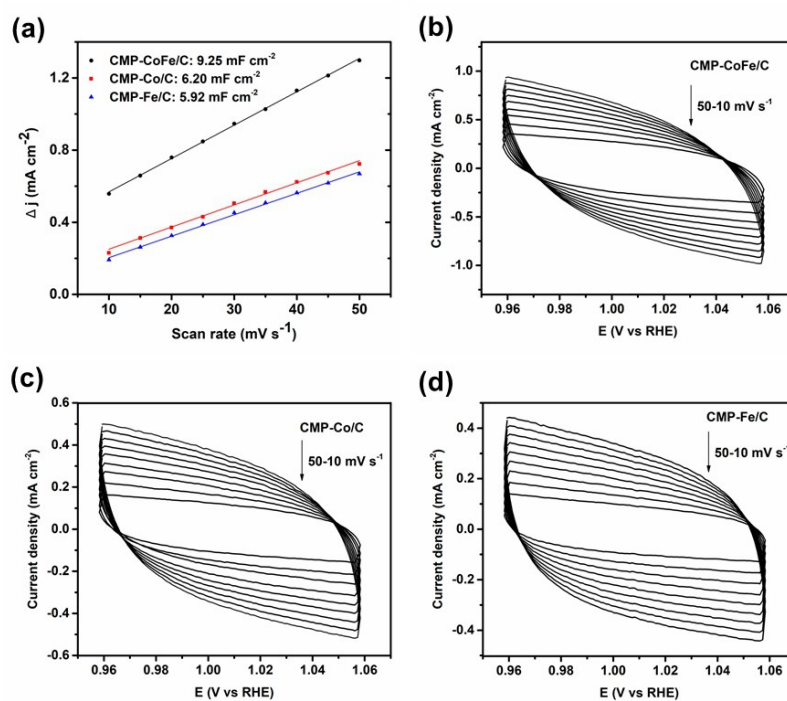


Fig. S10 (a) The capacitive current densities (measured at 1.01 V vs. RHE) against different scan rates. CV curves of CMP-CoFe/C (b), CMP-Co/C (c), and CMP-CoFe/C (d) at different scan rates ranging from 50 to 10 mV s⁻¹ with an interval of 5 mV s⁻¹.

Section 9. The LSV curve

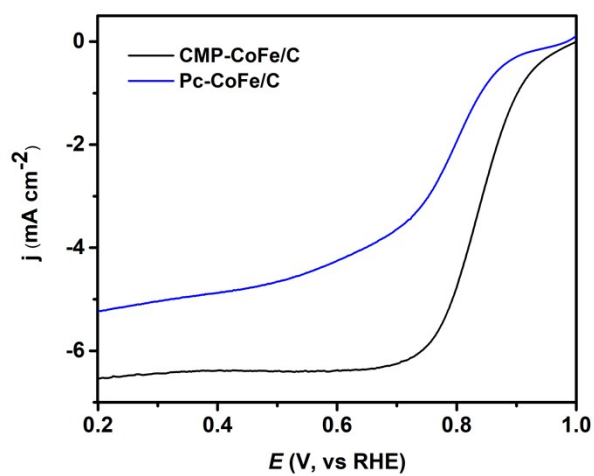


Fig. S11 LSV curves CMP-CoFe/C and Pc-CoFe/C in O₂-saturated 0.1 M KOH solution with 5 mV s⁻¹ scan rate using an RDE at 1600 rpm.

Section 11. Summary of bifunctional performance of related materials

Table S1 Comparison of bifunctional performance of reported catalysts and this work.

Catalyst	$E_{1/2}$ (V)	$E_{j=10}$ (V)	ΔE (V)	Refs
$\text{Ni}_x\text{Co}_{1-x}(\text{OH})_2$	0.62	1.56	0.96	[1]
$\text{NiFeO@MnO}_x(1:0.8)$	0.795	1.65	0.855	[2]
NiO/CoN Porous NW	0.68	1.53	0.85	[3]
Fe@N-C	0.84	1.70	0.86	[4]
NiCo/PFC aerogels	0.76	1.62	0.86	[5]
FeCo NPs doped carbon	0.92	1.73	0.81	[6]
Co@Co₃O₄/NC	0.80	1.65	0.85	[7]
Co-N_x-C graphene	0.80	1.75	0.95	[8]
FeNi-COP-800	0.803	1.63	0.827	[9]
CMP-CoFe/C	0.84	1.64	0.80	This work

References

- [1] L. Wang, C. Lin, D. Huang, F. Zhang, M. Wang, J. Jin, *ACS Appl. Mater. Inter.* **2014**, *6*, 10172–10180.
- [2] Y. Cheng, S. Dou, J. P. Veder, S. Wang, M. Saunders, S.P. Jiang, *ACS Appl. Mater. Inter.* **2017**, *9*, 8121–8133.
- [3] J. Yin, Y. Li, F. Lv, Q. Fan, Y. Q. Zhao, Q. Zhang, W. Wang, F. Cheng, P. Xi, S. Guo, *ACS Nano* **2017**, *11*, 2275–2283

- [4] J. Wang, H. Wu, D. Gao, S. Miao, G. Wang, X. Bao, *Nano Energy* **2015**, *13*, 387–396.
- [5] G. Fu, Y. Chen, Z. Cui, Y. Li, W. Zhou, S. Xin, Y. Tang, J. B. Goodenough, *Nano Lett.* **2016**, *16*, 6516–6522.
- [6] C. Y. Su, H. Cheng, W. Li, Z.-Q. Liu, N. Li, Z. Hou, F.-Q. Bai, H.-X. Zhang, T.-Y. Ma, *Adv. Energy Mater.* **2017**, *7*, 1602420.
- [7] A. Aijaz, J. Masa, C. Rösler, W. Xia, P. Weide, A. J. R. Botz, R. A. Fischer, W. Schuhmann, M. Muhler, *Angew. Chem. Int. Ed.* **2016**, *55*, 4087–4091.
- [8] C. Tang, B. Wang, H.-F. Wang, Q. Zhang, *Adv. Mater.* **2017**, *29*, 1703185
- [9] Z. Liao, Y. Wang, Q. Wang, Y. Cheng, Z. Xiang, *Applied Catalysis B: Environmental*, **2018**, *243*, 204–211.